

## Research



**Cite this article:** Farley FJM. 2018 The underwater resonant airbag: a new wave energy converter. *Proc. R. Soc. A* **474**: 20170192. <http://dx.doi.org/10.1098/rspa.2017.0192>

Received: 19 March 2017

Accepted: 19 June 2018

**Subject Areas:**

Ocean engineering, Power and energy systems

**Keywords:**

wave energy, numerical modelling, flexible bags

**Author for correspondence:**

Francis J. M. Farley

e-mail: [F.Farley@soton.ac.uk](mailto:F.Farley@soton.ac.uk)

# The underwater resonant airbag: a new wave energy converter

Francis J. M. Farley

Faculty of Engineering and the Environment, University of Southampton, Highfield, Southampton SO17 1BJ, UK

FJMF, 0000-0002-8077-7607

The time-domain simulation follows the heaving of the conical float in waves and calculates the bag shape, ballast motion, adiabatic air pressure and the flow through the turbine. There are two independent oscillators, the float with its resonance and the bag/ballast with its resonance. The coupling of the two oscillators gives rise to a wide band response with two peaks in the capture width each reaching the theoretical  $\lambda/2\pi$ . In this new wave energy converter, apart from the turbine, there are no mechanical moving parts, no joints nor pistons, no end stops nor sliding seals, no flaps nor one-way valves. The expected life of the airtight flexible bag remains to be determined, but potential manufacturers are optimistic.

## 1. Introduction

This paper describes a new concept in wave energy; an airbag filled with compressed air, underwater and ballasted, resonates with the waves. It is connected to a heaving float with its own more or less equal resonance. The coupling splits the resonance into two peaks, giving a broadband response.

A sealed flexible airtight fabric bag, entirely underwater, inflated with compressed air and ballasted to be neutrally buoyant, is unstable in heave. If it goes down the air is compressed, the buoyancy drops and the bag sinks further. It can be stabilized by a float of adequate water plane area attached to the top of the bag (figure 1). The instability of the bag then lengthens the natural heave period of the float.

If the top of the bag is fixed, still underwater, the ballast can rise and fall, shortening or lengthening the bag. The change in volume and air pressure then changes the tension in the fabric and the vertical force

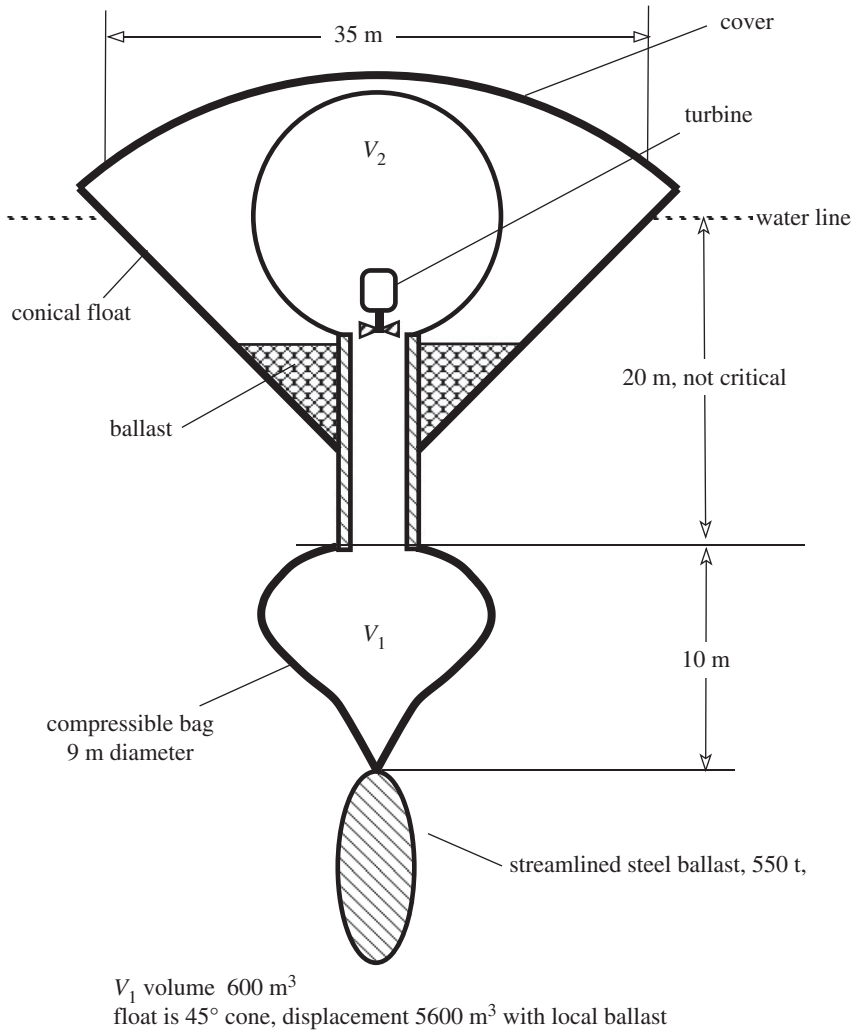


**Figure 1.** Conical float with underwater airbag.

on the ballast, generating a restoring force. In still water the ballast therefore oscillates in heave about its equilibrium position. The heave oscillation period of the ballast, with the top of the bag fixed, depends on the volume of the bag and the matching weight of the ballast. For example for a bag of  $550 \text{ m}^3$ , neutrally ballasted, the heave period of the ballast is  $8.7 \text{ s}$  and can resonate with the waves (figure 5). According to Froude scaling, for resonant period  $T$  the bag displacement and ballast weight are proportional to  $T^6$ .

By changing shape, the bag thus functions as an elastic spring, even if it is made of inextensible fabric. If the fabric can stretch then the effective spring constant of the bag will be reduced and the resonant period of the combination becomes longer; in this case, a smaller bag can resonate with the waves. In this paper, we consider only a bag which is flexible but longitudinally inextensible.

To support the ballast the tension in the fabric along lines of longitude must be large. The fabric is therefore reinforced vertically by a multiplicity of longitudinal tendons, for example, vectran straps integrated into the surface. Flexible fabric between the tendons makes the bag airtight. The material bulges outwards where the external water pressure is low, and bulges inwards lower down where the water pressure is high. Near the bottom, the fabric is folded inwards. These folds

and possibly some elasticity allow the fabric to follow the shape as the bag expands and contracts. The pressure difference across the fabric is small so the stress in the fabric is low. Underwater photos of the bag are given in figure 10.

The waves drive the float in heave. This motion is communicated to the top of the bag and excites a much larger resonant oscillation of the ballast. The change of pressure then drives air to and fro into another closed volume of air (referred to as  $V_2$ ), via a reversible flow turbine (Wells turbine) generating useful energy. There are two oscillators each with its own resonance; the float oscillating in heave, and the bag with its changing shape and the ballast oscillating below. The two oscillators are coupled and as in many physical systems this gives rise to two peaks in the response.

The system is complex with many coupled variables which need to be computed. The shape of the bag and its volume are affected by the air pressure inside, which in turn depends on the volume and the flow through the turbine. This changes the force on the ballast and its acceleration. The force at the top of the bag modifies the motion of the float engendered by the waves, which changes the drive on the bag; and so on.

Each variable is determined by a fairly simple equation, but the input parameters are changing and must be found from other equations. One can move forward using small steps in time. At each step a differential equation determines the new value of each variable, using the current values of the others. When all the variables have been recalculated one moves on to the next time step. In this way one maps the evolution of the whole system in time.

I have been using this method successfully since 1958 (originally to follow the three-dimensional spiral motion of charged particles in a non-uniform magnetic field [1]). The step in time is reduced until the final result is independent of the step length. Then simple equations apply and there is no need for complex interpolations, such as Runga–Kutta etc.

In [2], we reported an analysis of the same system using a linear frequency-domain model with many prior references and details of the experimental tests. The time-domain (real world) approach reported here provides a more immediate insight into the evolution of the variables, and reveals the nonlinearities which appear with larger waves. The objective of this paper is not to verify the calculation, which has been well established for a wide variety of systems, but to predict what can be realized with an underwater resonant airbag suspended below a heaving float. The calculations reported here are exploratory to see what might be achieved; at this stage, high accuracy is not needed. A large conical float (figure 1) is adopted for the computations because the hydrodynamic coefficients and added mass are known (see below). A more cost-effective float is illustrated in figure 12.

## 2. Hydrodynamic data

A good wave absorber must be a good wave radiator. In this case, the wave radiation comes primarily from the float. The bag is moving and changing volume, but being far underwater its wave radiation is assumed negligible. In [2, fig. 14], the radiation from the bag and the ballast are shown to be small. Observations of the ballast oscillation with an underwater camera show small damping also suggesting that the radiation is small.

A body with vertical sides does not displace water as it heaves, except at the bottom; and deep motion does not perturb the surface sufficiently. So a vertical sided body will not generate useful waves. To get good radiation the body should slope near the surface to push out water sideways. Therefore, we use a conical float. A rather flat cone with cone angle greater than  $45^\circ$  will radiate the most, but the water plane area will vary rapidly with depth. Tentatively, cone angle  $45^\circ$  is chosen for initial trials.

The added mass and radiation damping for conical floats of various angles have been calculated by Prof. John Chaplin at Southampton University (JR Chaplin 2013, unpublished data). Over a wide range the added mass is close to the mass of water displaced. The data on radiation can be fitted surprisingly accurately with a simple empirical formula which are convenient for calculations.

**Table 1.** Parameters for equation (2.2) for various cone angles.

| angle of cone to vertical (degrees) | $C$  | $\alpha$ | $\beta$ |
|-------------------------------------|------|----------|---------|
| 10                                  | 4.00 | 1.00     | 3.95    |
| 20                                  | 4.12 | 0.35     | 2.60    |
| 30                                  | 4.12 | 0.28     | 2.18    |
| 40                                  | 4.14 | 0.27     | 2.00    |
| 50                                  | 4.05 | 0.23     | 1.85    |
| 60                                  | 4.00 | 0.23     | 1.78    |
| 70                                  | 4.00 | 0.23     | 1.75    |
| 80                                  | 4.00 | 0.23     | 1.75    |

The radiation damping force  $F_r$  for a cone of water plane radius  $a$  heaving at angular frequency  $\omega$ , velocity  $v$  is

$$F_r = f \rho a^3 \omega v, \quad (2.1)$$

with the numerical coefficient  $f$  given by

$$f = C(x + \alpha x^4) \exp(-\beta x), \quad (2.2)$$

in which  $x = ka$  with  $k = 2\pi/\lambda$ . The values of the parameters  $C$ ,  $\alpha$ ,  $\beta$  which give a good fit to the cone data are shown in table 1. Interpolating, the values adopted for the  $45^\circ$  cone are  $C = 4.10$ ,  $\alpha = 0.25$ ,  $\beta = 1.92$ .

We also need the excitation force  $F_x$ , which is the vertical force on the cone for a wave of a given frequency and amplitude  $A$ . This is less than  $\rho g A$  times the water plane area, because the upward force is generated by the pressure on the sloping surface of the cone and the wave is attenuated with depth. Fortunately, we can use the Haskind relation which connects the excitation force on a body with its radiation damping. To get the correct capture width (CW), which should reach  $\lambda/2\pi$  at the peak of the resonance, the excitation force must match the damping force amplitude due to wave radiation, and this is what Haskind achieves. A good wave absorber is automatically a good wave radiator.

The radiation damping force  $F_r$  is proportional to the heave velocity  $v$  with the radiation coefficient  $b_r$  defined by

$$F_r = b_r v. \quad (2.3)$$

In deep water, the Haskind relation connecting  $b_r$  to the excitation force is

$$b_r = \left(\frac{F_x}{A}\right)^2 \frac{\omega^3}{2\rho g^3}, \quad (2.4)$$

in which  $F_x$  is the peak vertical force on the body for a wave of amplitude  $A$ . On the other hand, (2.1) for the cone implies

$$b_r = f \rho a^3 \omega. \quad (2.5)$$

Combining (2.4) and (2.5) gives the excitation ratio  $XF$

$$XF = \frac{F_x}{A} = \frac{g\rho}{k^2} \sqrt{2f(ka)^3}. \quad (2.6)$$

The radiation damping coefficient  $f$  and the excitation ratio  $XF$  both change with wave period according to equations (2.1) and (2.6) and this is included in the simulation.

### 3. Theory

The main difficulty in the calculation is finding the shape of the fabric in its vertical section. The bag is assumed to be isosymmetric about its vertical axis. The fabric and reinforcing tendons are inextensible, so the length of the fabric is fixed. The total force along the fabric at any level must be the same everywhere, otherwise the fabric will move. So the longitudinal tension  $F$  per unit horizontal width of fabric gets less where the bag is wide with large radius  $r$ , and  $q = Fr$  is constant. The radius of curvature  $R$  of the fabric in longitudinal section at any level is determined by the pressure difference  $\Delta p$  across the fabric,  $R = F/\Delta p$ . The tension along the horizontal cross section of the fabric is small and does not influence the general shape of the bag.

Assume that the depth  $z_0$  and radius at the top of the bag is defined by the float, while the depth  $z_{\text{bal}}$  and radius  $r_{\text{bal}}$  at the bottom of the bag is defined by the ballast. The air pressure  $p_1$  inside the bag is given. The value of  $q$  and the fabric angle  $\theta_0$  at the top are unknown. The calculation starts with assumed values for  $q$  and  $\theta_0$  and follows the fabric in equal steps along a line of longitude until it reaches the end. Then  $z_{\text{bal}}$  and  $r_{\text{bal}}$  will normally not match the desired end conditions, so the calculation must be repeated with modified values of  $q$  and  $\theta_0$ , until the fabric ends at the correct point. To speed the process, the effects of small steps in  $q$  and  $\theta_0$  are first calculated separately and the double adjustment is then made in a single move by using a standard  $2 \times 2$  matrix inversion.

When the fabric shape has been determined the vertical force on the ballast will, in general, not match its net weight, so the ballast will be accelerated and move to a new level. Because of resonance, the amplitude of the ballast oscillation can be much larger than the wave amplitude.

The volume  $V_1$  of the bag is recalculated with the corresponding air pressure  $p_1$  according to the adiabatic gas law  $pV^\gamma = \text{constant}$ . Any pressure difference ( $p_1 - p_2$ ) will then drive air through the turbine (assumed to be a linear resistance) into the second volume  $V_2$  with air pressure  $p_2$ ; the flow will change the pressure in the bag, to be used in the next time step. All these values vary as the machine operates and have to be recalculated at each time step.

For a given bag depth at the top  $z_0$  and at the bottom  $z_{\text{bal}}$  there is a unique solution which defines the fabric angle  $\theta_0$  at the top and the force on the ballast  $F_{\text{bal}}$ . Initially, this matches the net downward force  $M_{\text{bal}}$  on the ballast and the system is in equilibrium. But in general  $F_{\text{bal}}$  does not equal  $M_{\text{bal}}$  and the ballast is accelerated. As it moves the shape of the fabric is recalculated, the volume of the bag changes and the pressure inside is revised according to the adiabatic gas laws and the flow through the turbine into  $V_2$ .

At the top of the bag, the angle of the fabric generally differs from  $90^\circ$  (horizontal). The tension in the fabric then generates a vertical force  $F_{\text{top}}$  on the pipe connecting to the float above and this adds to the force of the waves.

If  $F_{\text{top}}$  opposes the float motion, the float does work on the bag, transferring energy to the ballast. This energy generates the flow of gas through the turbine and ultimately the useful power output. In its turn,  $F_{\text{top}}$  damps the motion of the float. The computer simulation in the time domain takes into account all these interconnected processes. Time advances in 2 ms steps. The shape of the bag, the gas pressure inside and the flow through the turbine are re-evaluated at each step. The turbine damps the gas flow and therefore the ballast oscillation which changes  $F_{\text{top}}$ . This, in turn, reacts on the float oscillation and reduces the waves radiated by the float.

As the bag is well below the surface the direct action of the waves on the bag is small and neglected. For the same reason, the wave radiated by the bag is not included. These assumptions have been confirmed in [2].

### 4. Coupled oscillators

In this system, there are two independent oscillators: (a) the float with its natural heave period and radiation damping, and (b) the bag/ballast system with its own resonance period determined by the size of the bag and the pressure inside, damped by the gas flow through the turbine. The

two oscillators are coupled by  $F_{\text{top}}$  which on one side drives the bag and on the other side reacts on the float. If the two systems are tuned to the same period, this coupling is enhanced.

Coupled oscillators occur in many branches of physics; superhet radios normally have two identical interconnected tuned circuits giving a desirable double-humped response. Other examples are the sodium D-lines, many quantum mechanical systems, as well as mechanical vibrations. In all cases, with initially equal periods the coupling splits the resonance into two separated peaks (normal modes). The stronger the coupling the further are the peaks driven apart.

## 5. Simulation

In the simulation, monochromatic incident waves drive the conical float, which in turn sets up an oscillation of the ballast. This drives air to and fro, into and out of  $V_2$ , through the turbine which is represented by a linear resistance with the volume flow in  $\text{m}^3 \text{s}^{-1}$  proportional to the pressure drop in metres head. The ratio of flow in  $\text{m}^3 \text{s}^{-1}$  per metre of pressure head is referred to as  $ftv$ . The pneumatic energy input to the turbine is accumulated and compared with the incident wave energy per metre wavefront. This gives the CW. The added mass is included for the float and the ballast.

At each step in time the calculation follows a number of interconnected variables:

- the elevation of the float, including the wave force and the force from the top of the bag
- the shape of the bag, volume and pressure inside  $p_1$
- the force on the ballast, ballast acceleration, velocity and position
- the mass flow through the turbine to  $V_2$ , with its internal pressure  $p_2$
- pneumatic energy transferred to the turbine
- increase the time  $t$  to  $t + \delta t$  and recycle.

We make each calculation in turn, using the latest values of the other variables which may, however, be out of date by one time step  $\delta t$  (typically 2 ms). If the step in time is short enough the error will be negligible. The pressures  $p_1$  and  $p_2$  are calculated using the adiabatic relation  $pV^\gamma = \text{constant}$ , adjusted for the mass of the gas in volumes  $V_1$  and  $V_2$  if this has changed due to flow through the turbine. Heat exchange with the walls of the vessels is assumed to be negligible; surely true on the full scale, may not be true for small models. The net downforce on the ballast (allowing for buoyancy) at equilibrium is equal to the upthrust on the bag volume. The ballast is ellipsoidal so its added mass is equal to the mass of water displaced. The added mass of the cone, calculated by Chaplin (JR Chaplin 2013, unpublished data), is close to the mass of water displaced.

For the complete system, the CW versus wave period  $T$  is given in figure 2. The bag/ballast system is rather nonlinear, so its resonant period changes with ballast amplitude and with large motions we do not get a good resonance (figure 3). Therefore, I am computing the performance in small waves. For this example, the cone diameter at the water line is 35 m and its displacement 5600 t, bag displacement is 550 t and the volume ratio  $V_2/V_1 = 3$ . Both oscillators are tuned close to 9 s waves. We see that the resonance is split into two peaks. With the optimum value of turbine flow ( $ftv = 14 \text{ m}^3 \text{ s}^{-1}$  per m head) both reach the theoretical value of  $\lambda/2\pi$ . This is only achieved with small waves and using Haskind to match the excitation force with the radiation damping. We cannot change the coupling force  $F_{\text{top}}$ , so the separation of the peaks is out of our control. Luckily it broadens the resonance more or less optimally.

The response for larger wave amplitudes is shown in figure 3. Wave amplitude 0.5 m gives a good response; but for amplitude 1 m the CW drops by a factor of about 2.5 because the bag has limited volume and cannot pump enough air. This drop may be larger than we would wish, but in general, the limitation of output power in large waves is to be welcomed. Prof. R.C.T. Rainey [3] for example has consistently emphasized the value of nonlinearity in protecting wave energy converters from damage. One could double the volume of the bag so that it can pump more, and this would increase the resonance period by only 12%. Alternatively to double the pumping

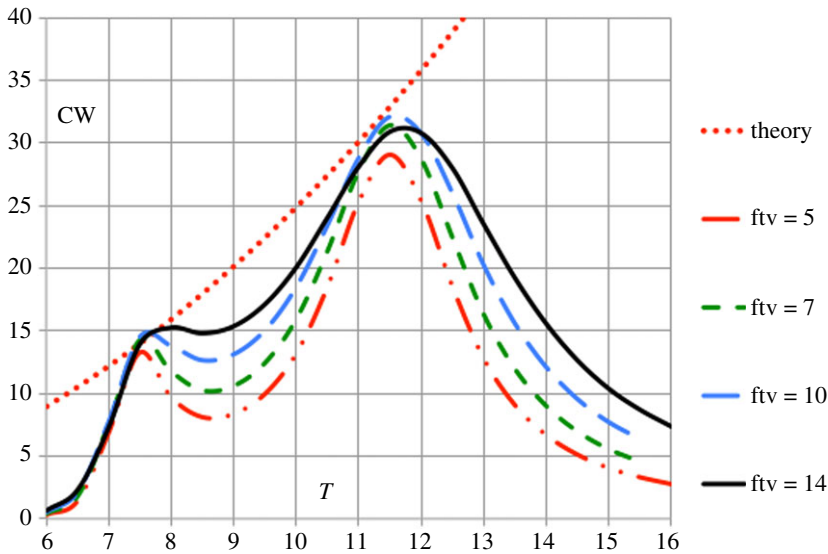


**Figure 2.** CW in metres versus wave period in seconds, for various turbine flows  $ftv$  in  $m^3 s^{-1}$  per metre water head, wave amplitude = 0.02 m. The dotted line gives the theoretical maximum  $CW = \lambda / 2\pi$ . (Online version in colour.)

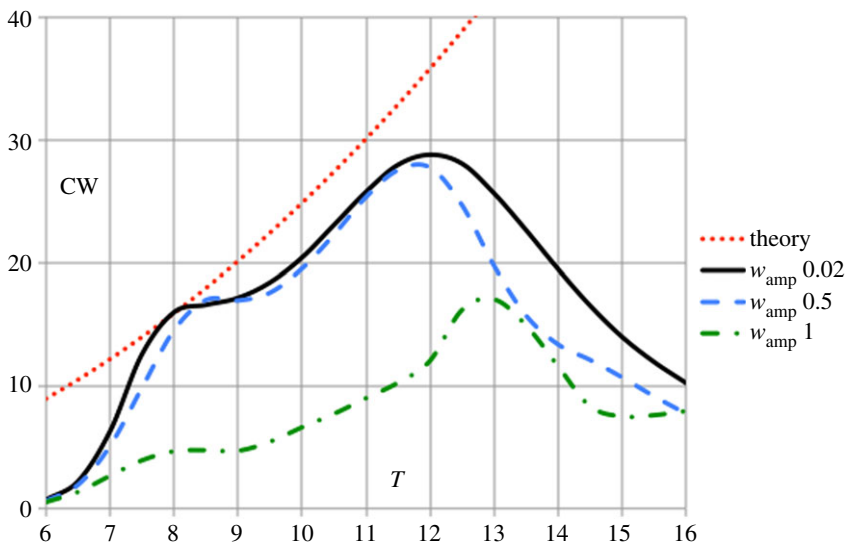


**Figure 3.** CW versus wave period, for wave amplitudes 0.02, 0.5 and 1.0 m,  $ftv = 20$ . (Online version in colour.)

volume furnish the float with two identical bags. The volume of  $V_2$  would have to be increased *pro rata*. These options could be considered.

Figures 4 and 5 show the damped oscillations of each system excited separately and uncoupled. In each case, the oscillation was started by applying an arbitrary upward velocity to the plotted variable. The decay of the oscillations corresponds to  $Q$ -values of 2.58 for the float due to the radiation damping and 2.64 for the ballast due to the flow through the turbine at the optimum value of  $ftv$ . It is remarkable that with the optimum power take off damping, chosen from figure 2, the  $Q$ -values of the two oscillators are almost equal.

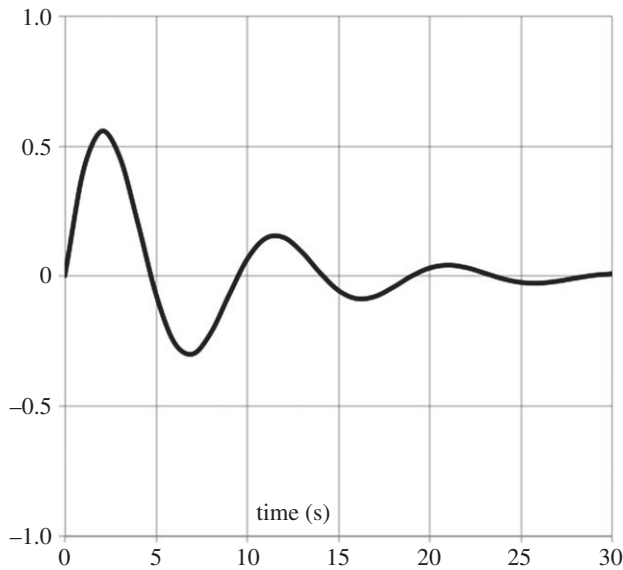


**Figure 4.** Damped oscillation of the float by itself, period 9.9 s,  $Q$ -value 2.6. Vertical displacement in metres.

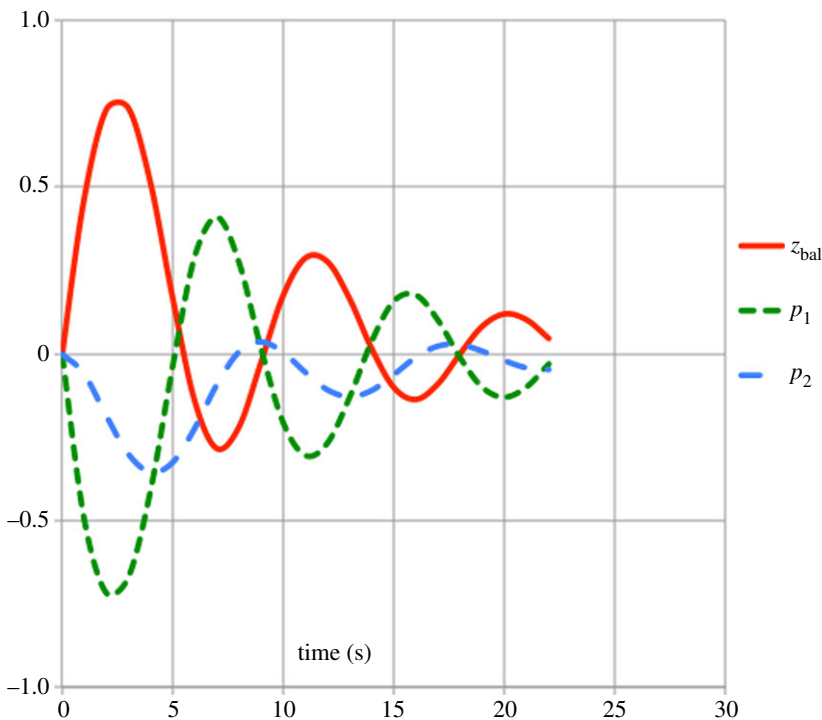


**Figure 5.** Damped oscillation of the ballast by itself (red) at the optimum  $ftv = 14$ . Period is 8.7 s,  $Q$ -value 2.6. Vertical displacement in metres. Also shown is the pressure  $p_1$  in  $V_1$  (green) and the pressure  $p_2$  in  $V_2$  (blue). The phase lag is due to the flow. Pressures in metres head. (Online version in colour.)

Figures 6 and 7 show the time sequence of movements and pressures for two wave periods,  $T = 8$  s and  $T = 11.5$  s, that is at the lower and upper peaks in the CW response (figure 2). For 8 s waves (figure 6), the ballast amplitude (red solid) is about 2.5 times the wave excitation force amplitude

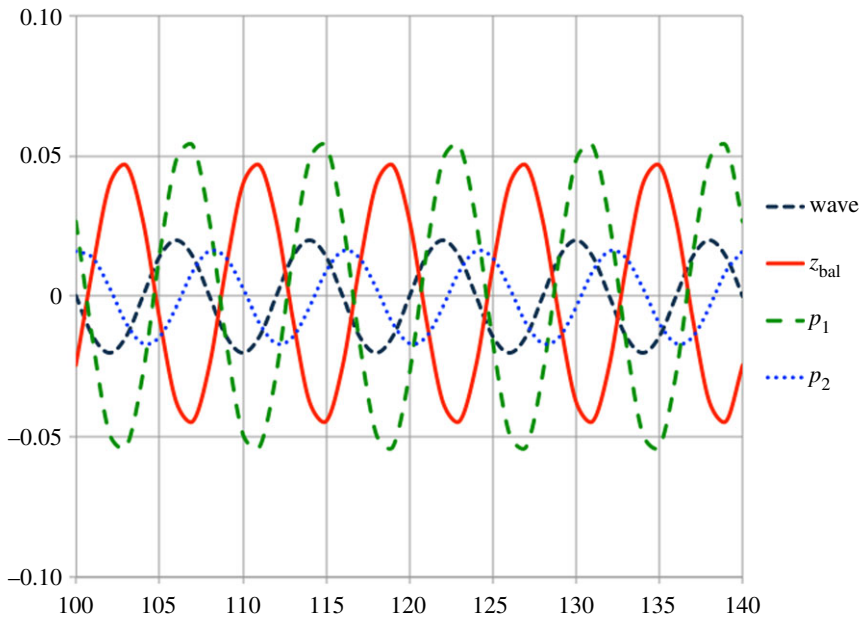


**Figure 6.** Time sequence for wave period 8 s. Displacements and pressures in metres head are plotted versus elapsed time in seconds. Line labelled ‘wave’ is the excitation force on the float due to the wave. (Online version in colour.)

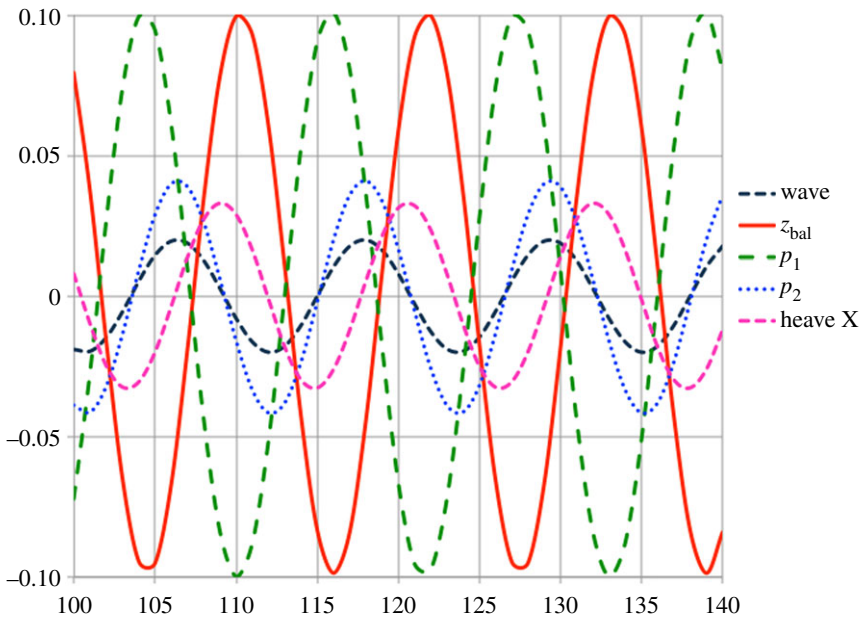


**Figure 7.** Time sequence for wave period 11.5 s. Displacements and pressures in metres head are plotted versus elapsed time in seconds. ‘wave’ is the excitation force, ‘heave X’ is the displacement of the float. (Online version in colour.)

(black, dashed). Pressure  $p_1$  in the bag (green, long dash) tracks the ballast with opposite phase, while the pressure  $p_2$  in  $V_2$  (blue dotted) is smaller and lags about  $45^\circ$  on  $p_1$ .

For 11.5 s waves (figure 7), the curves are similar but with larger amplitudes. When the ballast (orange solid) is up, the fabric is pressing upwards on the float so  $F_{\text{top}}$  (not plotted) is in antiphase

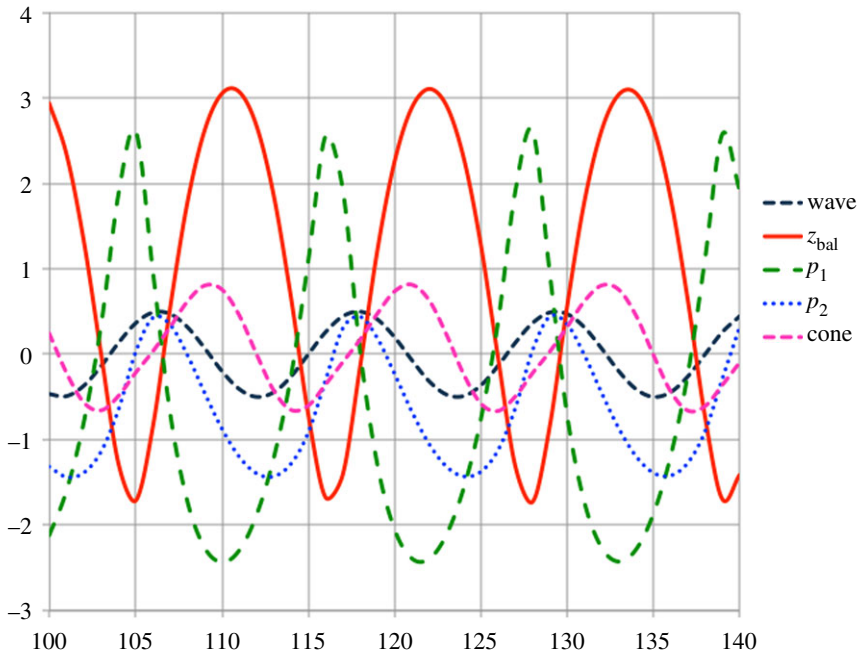


**Figure 8.** Time sequence for wave period 11.5 s with larger wave amplitude 0.5 m. Displacements and pressures in metres head are plotted versus elapsed time in seconds. (Online version in colour.)

with the wave excitation force on the cone (black dashed). Therefore, the heave amplitude of the cone (pink long dash) is only slightly larger than the wave force. The cone motion lags relative to the wave, as required to transfer energy and radiate a wave in antiphase with the incoming wave.

In figure 8, the amplitude of the 11.5 s waves was increased to 0.5 m and nonlinearity is starting to distort the waveforms. The reaction force applied to the cone by the bag,  $F_{\text{top}}$  (not plotted), is about one-tenth of the wave force on the cone (black, dashed).

The displacement of the cone is the pink dashed line. When the cone has its maximum downward velocity,  $F_{\text{top}}$  is large and positive. Conversely, when the cone is moving upwards  $F_{\text{top}}$  is maximally negative. So  $F_{\text{top}}$  reduces the cone velocity and damps its motion;  $F_{\text{top}}$  also transfers energy from the cone to the bag. The force on the cone due to radiation damping (not plotted) is of the same magnitude as  $F_{\text{top}}$ , (as it should be to get optimum CW) and together they delay the cone motion (pink dashed) so that it lags  $90^\circ$  on the wave.

It is the motion applied to the top of the bag by the cone (red dashed) that drives the bag oscillation. The motion of the ballast (orange) follows with almost one-quarter of a cycle delay.

The heave amplitude of the cone (red dashed) is 1.3 times the wave amplitude (black dashed) but the ballast amplitude is 4.5 times the wave. The ballast motion (red) is no longer sinusoidal but has a narrow downward peak; correspondingly the pressure  $p_1$  (green) in the bag has a narrow positive peak. The pressure excursion in the bag (green dashed) is  $\pm 5$  times the wave amplitude. The pressure across the turbine ( $p_1 - p_2$ ) is about five times the wave amplitude. Note that when the pressure  $p_2$  in  $V_2$  (blue dotted) is equal to  $p_1$  the flow through the turbine drops to zero so  $p_2$  is at its maximum or minimum.

## 6. Bag shape

The changing shape of the bag is shown in figure 9 for waves of 11 s period and amplitude 1 m. The range of ballast motion is 7 m, while the top of the bag (attached to the cone) moves only about 2 m. (For the relative phase of the top and bottom motions, figure 8). It is the top motion that drives the ballast, but there is a complex and varying phase delay between them. The response is

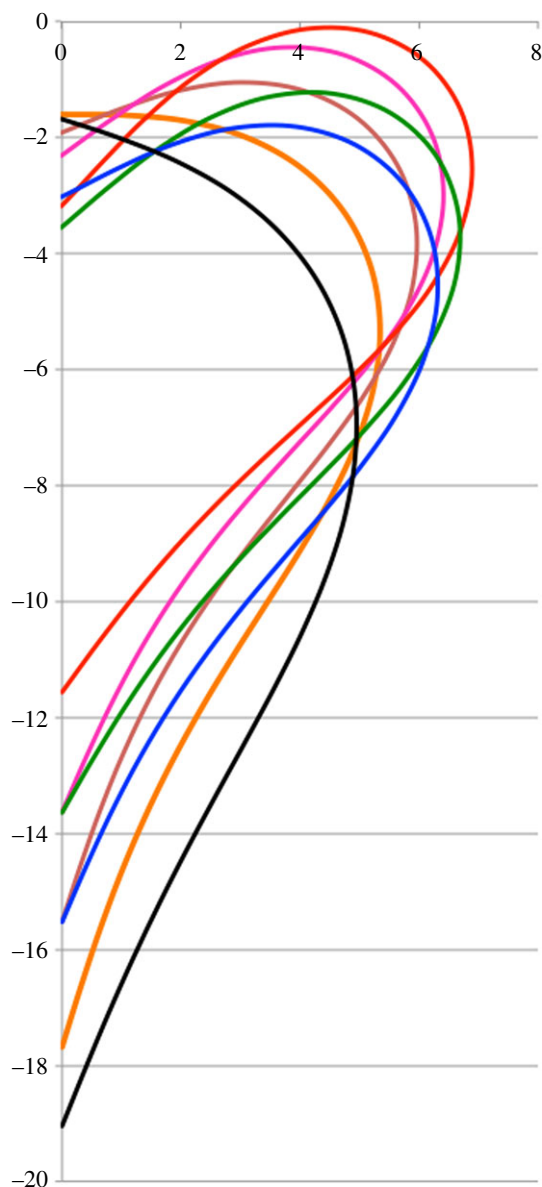


**Figure 9.** Bag shapes for wave period 11 s, and wave amplitude 1 m. The bag is axisymmetric about the vertical axis: the calculated vertical section of one half of the bag is plotted. Horizontal and vertical scales in metres. When the ballast is low (black line) the bag is narrow and thin, minimum volume; when the ballast is high (red line) the bag is heart-shaped, maximum volume. (Online version in colour.)

already becoming substantially nonlinear for this wave amplitude. Underwater photos of the bag are given in figure 10.

## 7. Tests

In model tests, it is necessary to correct for the compressibility of air which is much smaller at the reduced scale. This is normally done by adding large volumes of air, for example to  $V_1$  and  $V_2$ . It is easier to make the model volumes appropriately distensible, thus allowing more space for the incompressible model air (Farley FMJ 2015, unpublished data). The distensibility of the model volumes then tracks the compressibility of the full-scale gas.

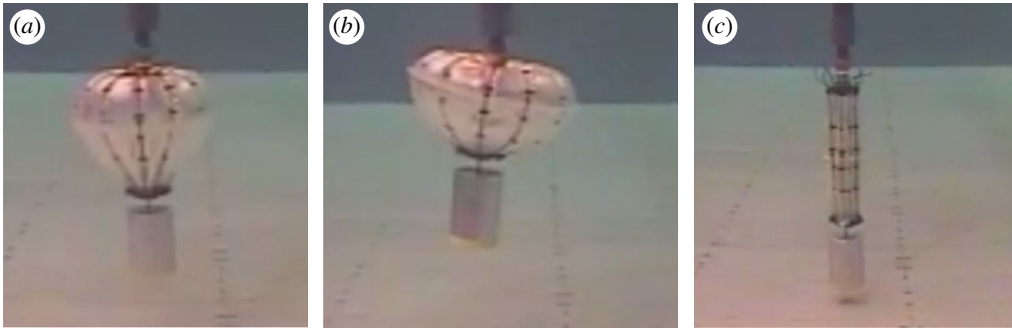


**Figure 10.** Underwater photos of the bag, (a) ballast low, bag compressed, (b) ballast high, bag expanded, (c) no air pressure, bag collapses, no air is pumped. (Online version in colour.)

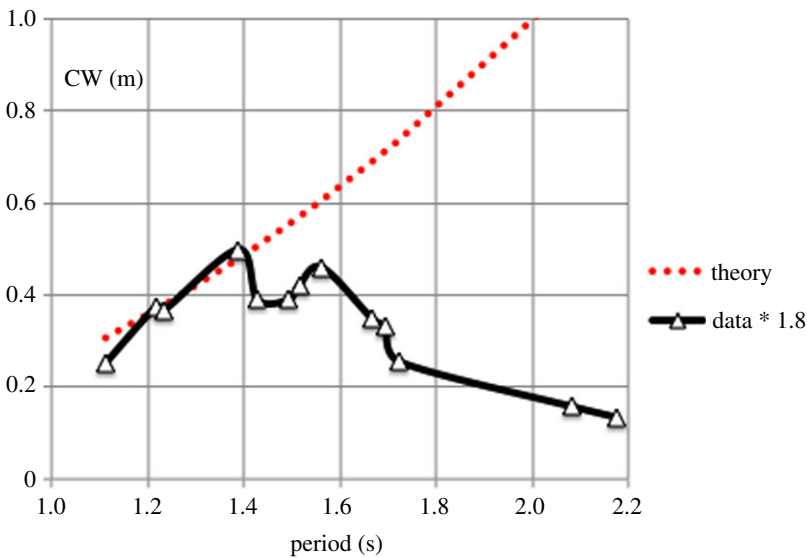


**Figure 11.** Model capture widths CW versus wave period  $T$  (black solid) for wave amplitude 3 cm. Red dotted line  $CW \lambda/2\pi$  divided by 1.8. (Online version in colour.)

Model tests with a bag mounted below a 1 m diameter  $45^\circ$  cone were carried out at Plymouth University [2] with wavelengths around 3 m and amplitude 0.03 m. A selection of the data from these tests (not included in [2]) are shown in figure 11 (black solid). According to figure 3, nonlinear effects in the bag are to be expected with this ratio of amplitude to wavelength (1 in 100), so the CW was considerably less than theory. Therefore, for easy comparison the theoretical CW  $\lambda/2\pi$  (red dotted) has been divided by 1.8. Fluctuations due to measurement errors are apparent but the wide response predicted in figure 2 is generally confirmed and there is some indication of the expected double peak. Future tests with smaller waves would be of interest, but with small waves errors can arise from random residual motions in the tank. Ideally, we need to move up to a larger scale.

Using figure 11 and scaling up from 1.4 s to 10 s waves in the sea, the wave amplitude would be 1.5 m and the wave power  $88 \text{ kW m}^{-1}$ . With CW equal to theory divided by 1.8, that is 14 m, the captured pneumatic power would be 1.2 MW. With turbine efficiency 50% this would give an average power output of 600 kW. Although the CW is below theory for large waves, the output would nevertheless be useful.

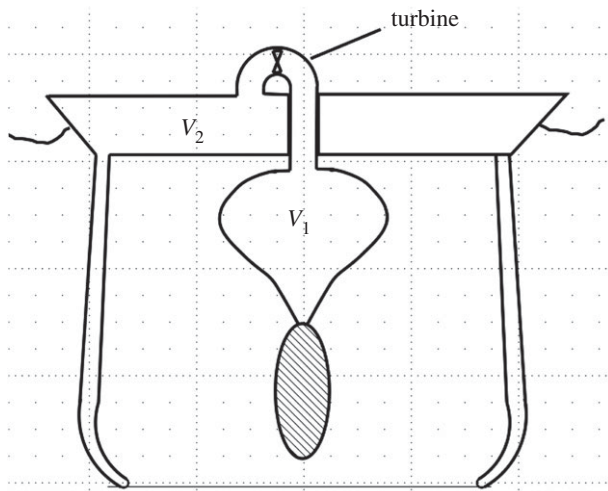


**Figure 12.** Wave bell. The bag is suspended inside a bell-shaped float which has high inertia from the enclosed water. Any trapped air vents to atmosphere through a small pipe not shown.

## 8. Discussion

The CW versus wave period ( $T$ ) was calculated in [2] using the linear frequency-domain model and plotted in figs. 10, 12 and 13 of that paper. The separated peaks due to the coupling of the two oscillators are clearly seen. With optimum parameters (fig. 13), both peaks reach  $\lambda/2\pi$  and the ratio of the peak periods is about 1.6, agreeing with figure 2 of this paper.

However [2] already revealed the importance of the nonlinearities in the bag. The ‘S-shaped curve’ of bag shape versus internal pressure (figure 11) is itself due to this nonlinearity. The graphs of CW versus wave period in figure 12 depend critically on the start point. As the bag shape changes in the real world, the performance will be some average which is hard to determine. By contrast, the time-domain method automatically follows any changes in parameters due to nonlinearities as they arise. See, for example, figure 8 in which the wave excitation force is far from sinusoidal. The time-domain method used here will make better predictions.

The device dimensions used here are an example to illustrate the principle. They have not been optimized for a particular wave climate. Commercial optimization to obtain the best yield to cost ratio would depend on many factors which have not been considered. In figure 1, the float is 35 m diameter at the waterline, has displacement 5600 t, which is rather large. Ballast is cheap but this float could be too expensive.

An alternative design, the wave bell, with less structure and less depth, is illustrated in figure 12. The float is shallow and incorporates the fixed air volume  $V_2$ . At the waterline, the edge of the float is conical to radiate waves and increase the radiation damping. The float is provided with a deep underwater skirt [4]: this traps a volume of water which must heave with the float and therefore adds inertia, lengthening the heave period (verified experimentally). The flexible airbag located inside the skirt is protected from the waves and can hardly radiate beyond the bell. The hydrodynamic coefficients of this structure have not been calculated at this stage. They can easily be adjusted. Increasing the float diameter decreases the resonance period and increases the damping. Increasing the depth of the skirt lengthens the resonance period.

One or two underwater bags may be attached to an elongated float which pitches in the waves. A pitching wave energy converter can have a CW of  $2 \times \lambda/2\pi$  and with the correct combination of pitch and heave [5,6] the CW can rise to  $3 \times \lambda/2\pi$ , about 70 m in 10 s waves, giving an attractive power output in a single device. Many such options remain to be explored.

## 9. No moving parts

Most wave energy converters have mechanical moving parts, hinges, joints, pistons, end stops, sliding seals, flaps or one-way valves. When deployed in realistic conditions all these have failed. Apart from the turbine, this machine has no mechanical moving parts whatsoever. The only question is the life of the bag. This needs to be studied, but manufacturers are optimistic. In any case, if the bag fails there is sufficient reserve buoyancy in the float to support the ballast, and the turbine can be mounted above the waterline. Replacing a bag should not be a major expense.

## 10. Survival

In heavy weather, the bag can be deflated as in Figure 10c. It then collapses and no longer pumps air. This will protect the turbine. For more protection, the whole machine can easily be sunk in storms by flooding the float and stabilized at some suitable depth. The system is completely sealed and under pressure, so no water can enter. Reinflating with air pumped through a snorkel or from cylinders restores the operation.

## 11. Conclusion

The underwater resonant airbag is a new concept for wave energy conversion [7]. According to the simulations and tests it works well. Apart from the reversible flow turbine, the device has no mechanical moving parts requiring lubrication. It has a good CW with wide-band response. It appears to be inexpensive. The life of the flexible underwater bag needs to be tested but possible manufacturers are optimistic. The underwater resonant airbag can be used as wave power take off for any floating device with vertical motion.

**Data accessibility.** This paper has no data. Prof. Chaplin's results on radiation coefficients and the added mass of conical floats are not in the public domain. Equation (2.2) and the parameters of table 1 are included in the hope that they may be useful for users of conical floats.

**Competing interests.** I have no competing interests.

**Funding.** This work is entirely self-funded.

**Acknowledgements.** Many thanks to Prof. John Chaplin for calculating the radiation coefficients and added masses of cones. Thanks to him also, with Deborah Greaves, Martyn Hann and A. Kurniawan, for testing a model in the COAST wave tank at Plymouth University as described in [2]. I am also very grateful for the efforts of the referees, whose comments have led to significant improvements in the paper.

## References

1. Farley FJM. 1959 Computation of particle trajectories in the CERN cyclotron. CERN yellow report 59-12.
2. Kurniawan A, Chaplin JR, Hann MR, Greaves DM, Farley FJM. 2017 Wave energy absorption by a submerged air bag connected to a rigid float. *Proc. R. Soc. A* **473**, 20160861. (doi:10.1098/rspa.2016.0861)
3. Rainey RCT. 2012 Key features of wave energy. *Phil. Trans. R. Soc. A* **370**, 425-438. (doi:10.1098/rsta.2011.0251)
4. Farley FJM. 2017 Wavebell - a new wave energy converter. See <http://www.wavebell.org>.
5. Falnes J. 2002 *Ocean waves and oscillating systems*, pp. 216-217. Cambridge, UK: Cambridge University Press.
6. Farley FJM. 2012 Far field theory of wave power capture by oscillating systems. *Phil. Trans. R. Soc. A* **370**, 278-287. (doi:10.1098/rsta.2011.0275)
7. Farley FJM. 2014 Wave power converter, patent GB 2532074, 9 Nov 2014. PCT/GB2015/053377.